06

The epitaxy of AlN(11$\bar{2}$2)-layers on GaN(11-22)/m-Al2O3

© V.N. Bessolov[1], E.V. Konenkova[1], A.V. Kremleva[2], L.A. Sokura[1,2], S.S. Sharofidinov[1], M.P. Scheglov[1]

[1] Ioffe Institute, St. Petersburg, Russia
[2] ITMO University, St. Petersburg, Russia
E-mail: lena@triat.mail.ioffe.ru

Received April 7, 2025
Revised June 2, 2025
Accepted June 5, 2025

The epitaxial layers of AlN(11$\bar{2}$2) with a thickness of 3.9 μm were grown on a GaN(11$\bar{2}$2)/*m*-Al_2O_3 template by hydride vapour-phase epitaxy (HVPE). The template consisted of GaN(11$\bar{2}$2)- and buffer AlN s with thicknesses of 2.7 m and 0.6 μm, respectively, grown on a sapphire substrate of orientation (10$\bar{1}$0). It is shown that the full width at half maximum (FWHM) for the diffraction peaks of GaN(11$\bar{2}$2)/*m*-Al_2O_3 and AlN(11$\bar{2}$2) are 30 and 20 arc minutes, respectively. It was found that the epitaxy of AlN(11$\bar{2}$2) on the template leads to an increase in the size of crystal blocks in the AlN(11$\bar{2}$2) layer. It is assumed that the improvement in the quality of the AlN(11$\bar{2}$2) layer occurs due to its predominant growth in the tangential direction due to the relatively low lattice difference at the AlN(11$\bar{2}$2)/GaN(11$\bar{2}$2) heterogeneous boundary.

Keywords::semipolar AlN(11$\bar{2}$2), hydride vapour-phase epitaxy.

DOI: 10.61011/TPL.2025.08.61553.20336

Aluminum nitride (AlN) has great potential for application in optoelectronic devices operating in the deep ultraviolet range and in high-power and high-frequency electronic devices, since it has a wide band gap and fitting properties [1]. However, strong spontaneous and piezoelectric polarization in the [0001] direction of aluminum nitride reduces the overlap of the electron and hole wave functions and exerts a negative influence on the electron recombination efficiency. This obstacle may be cleared through the use of non-polar or semi-polar layers. However, it is extremely difficult to grow high-quality semi-polar AlN due to the low migration activity of aluminum atoms on the surface, which inevitably leads to a columnar growth mode and a rough surface. Several methods for improving the quality of crystalline polar and semi-polar epitaxial AlN layers, such as high-temperature growth [2], sapphire nanostructuring [3], or preliminary nitridation of the sapphire substrate [4], have been developed. It is rather difficult to grow layers with a smooth surface due to the strong anisotropy of non-polar and semi-polar AlN [5].

The use of AlN(10$\bar{1}$1), AlN(10$\bar{1}$3), and AlN(11$\bar{2}$2) layers in device structures for suppression of the influence of internal electric fields is a promising trend in optoelectronics [6]. Numerous studies focused on improving the quality of semi-polar AlN on sapphire have been published over the last two decades, and the possibility of synthesis of layers with different semi-polar surface orientations has been demonstrated [7]. The growth of high-quality AlN layers by metal-organic chemical vapor deposition (MOCVD) and hydride vapor-phase epitaxy (HVPE) with magnetron sputtering of AlN on sapphire as a buffer layer has recently been reported in [8].

In the present study, we propose a new approach to HVPE synthesis of AlN(11$\bar{2}$2) layers on a sapphire substrate with the (10$\bar{1}$0) surface orientation with micrometer-sized GaN(11$\bar{2}$2) layers used as a template.

Let us note first that AlN(11$\bar{2}$2) layers may be formed on an *m*-Al_2O_3 substrate by heating in a gas environment with excess ammonia. This is made possible by the formation of nanofacets on *m*-sapphire at high temperature [9]. AlN(11$\bar{2}$2) layers were synthesized as follows. Heteroepitaxy was performed on sapphire substrates of the (10$\bar{1}$0) orientation cleaned in advance in the standard way. A buffer layer of AlN with a thickness of 0.6 μm was grown first in an argon atmosphere, which was followed by the synthesis of a 2.7-μm-thick GaN layer. At the last stage, the main layer of AlN with a thickness of 3.9 μm was formed (Fig. 1). The flow rates of HCl and NH_3 were 1.7 and 2.4 l/min, respectively. The temperature of epitaxy of AlN

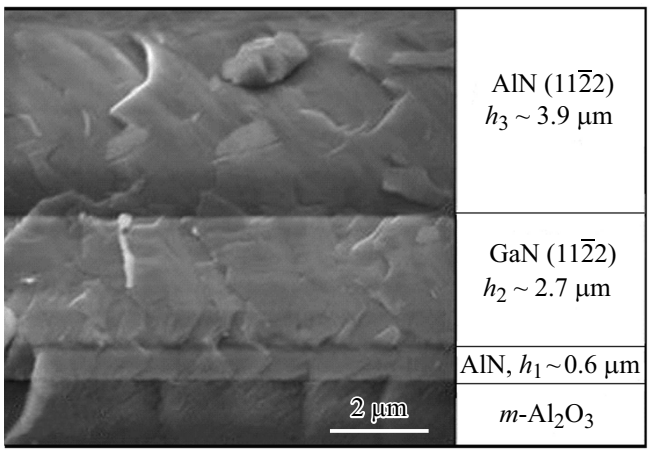

Figure 1. SEM image of the cleaved surface of an AlN(11$\bar{2}$2) layer with template GaN(11$\bar{2}$2)/*m*-Al_2O_3.

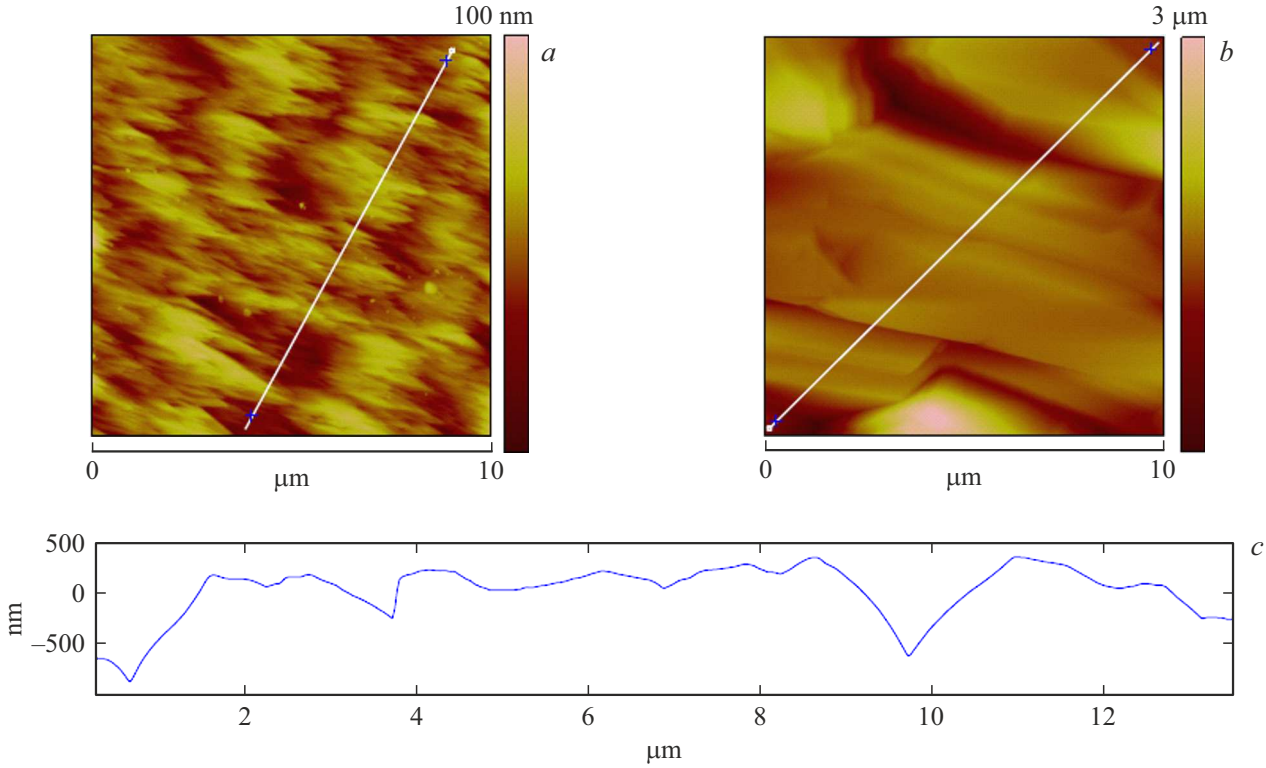

Figure 2. AFM images (*a*, *b*) and profile (*c*) of the surface of GaN(11$\bar{2}$2)/*m*-Al_2O_3 (*a*) and AlN(11$\bar{2}$2)/GaN(11$\bar{2}$2)/*m*-Al_2O_3 (*b*, *c*) structures.

Table 1. FWHM of X-ray diffraction ω_θ, root-mean-square value (RMS), and average roughness R_a for a semi-polar AlN(11$\bar{2}$2) layer and a GaN(11$\bar{2}$2)/*m*-Al_2O_3 template with scanning over 1×1 and $10 \times 10\,\mu$m areas

Substrate	ω_θ, arcmin	RMS, nm		R_a, nm	
		1×1	10×10	1×1	10×10
GaN(11$\bar{2}$2)/*m*-Al_2O_3	30	1.65	11.2	1.26	8.87
AlN(11$\bar{2}$2)/GaN(11$\bar{2}$2)/*m*-Al_2O_3	20	2.35	116	1.38	85.5

and GaN layers was close to 1000 and 1050 °C, respectively. The approximate time of epitaxial layer growth was 15 min.

The structural and optical characteristics of GaN and AlN layers of these structures were determined using X-ray diffractometry and optical, scanning electron (SEM), and atomic force (AFM) microscopy. In X-ray measurements, rocking curves were recorded in a double-crystal diffraction arrangement in reflections (0002) and (11$\bar{2}$2) of Cu$K_{\alpha 1}$ radiation using a triple-crystal X-ray spectrometer.

Nitridation of the *m*-Al_2O_3 substrate at $T = 1000$ °C provided an opportunity to grow a low-quality AlN buffer layer consisting of blocks, some of which have the AlN(11$\bar{2}$2) orientation. Partial orientation of the buffer layer in the semi-polar direction allowed us to grow GaN(11$\bar{2}$2) and AlN(11$\bar{2}$2) layers.

X-ray diffraction measurements revealed that the full width at half maximum (FWHM) of X-ray rocking curves for the GaN(11$\bar{2}$2) and AlN(11$\bar{2}$2) diffraction peaks is 30 and 20 arcmin, respectively.

AFM imaging of GaN(11$\bar{2}$2) layers and, after further growth, AlN(11$\bar{2}$2) layers demonstrated that the surface of both layers consists of elongated domains (Fig. 2). It was found that small domains $2 \times 4\,\mu$m in size on the surface of the GaN(11$\bar{2}$2) layer merged in the course of further growth of AlN, dwindling in number and increasing in size to $8 \times 20\,\mu$m, and higher-quality AlN(11$\bar{2}$2) layers were formed. Compared to GaN(11$\bar{2}$2), the root-mean-square (RMS) and average (R_a) roughness values of the AlN(11$\bar{2}$2) layer surface increased slightly when scanning over an area of $1 \times 1\,\mu$m and differed significantly at $10 \times 10\,\mu$m (Table 1).

As is known, the AlN orientation on *m*-plane sapphire in gas-phase epitaxy may change either to (10$\bar{1}$3) or to (11$\bar{2}$2) depending on the concentration of NH_3 in the gas phase and the temperature [9]. This is attributable to the possible formation of *r*-plane nanofacets on *m*-plane sapphire in the case of its nitridation and at a relatively high temperature, which lead to growth of the (11$\bar{2}$2) plane.

Table 2. Lattice parameter a at room temperature [10] and relative mismatch $\Delta a/a$ at the heteroboundary

Lattice parameter a, Å					Lattice parameter mismatch $\Delta a/a$	
m-Al_2O_3	GaN	AlN	GaN(11$\bar{2}$2)	AlN(11$\bar{2}$2)	GaN(11$\bar{2}$2)/m-Al_2O_3	AlN(11$\bar{2}$2)/GaN(11$\bar{2}$2)
4.785	3.189	3.112	5.517	5.390	0.128	−0.024

According to the results of X-ray diffraction studies, the semi-polar orientation of the buffer layer cannot be established, apparently due to the polycrystalline nature of the buffer layer resulting from a significant difference in lattice parameters of m-Al_2O_3 and AlN (Table 2).

We associate the effect of growth of AlN(11$\bar{2}$2) blocks with the difference in magnitude of the lattice parameter mismatch at the GaN(11$\bar{2}$2)/m-Al_2O_3 and AlN(11$\bar{2}$2)/GaN(11$\bar{2}$2) heteroboundaries (Table 2). The relative magnitude of mismatch at the heteroboundary may be estimated as $\Delta a/a = (a_1 - a_2)/a_2$, where a_1 and a_2 are the lattice parameters of two adjacent layers at the heteroboundary (Table 2) [10]. We believe that the large lattice mismatch at the AlN(11$\bar{2}$2)/m-Al_2O_3 and GaN(11$\bar{2}$2)/m-Al_2O_3 heteroboundaries leads, first, to the formation of a fine-grained polycrystalline AlN buffer layer and, second, to the formation of a layer of semi-polar gallium nitride with block sizes of about $2\,\mu$m in the [1$\bar{1}$00] direction (see Fig. 2, *a*). When the AlN(11$\bar{2}$2) layer is formed on the GaN(11$\bar{2}$2)/m-Al_2O_3 template, the lattice mismatch in this direction is significantly smaller (Table 2). This leads to the growth of a layer with larger blocks by HVPE in an argon atmosphere (Figs. 2, *b*, *c*). The FWHM for diffraction peaks of the template and the AlN(11$\bar{2}$2) layer was found to be 30 and 20 arcmin, respectively, which is close to similar diffraction data for the AlN(11$\bar{2}$2) layers grown on (10$\bar{1}$0) sapphire substrates by MOCVD [11].

The results demonstrate the potential of the method for fabrication of stripe templates for micrometer-sized semi-polar optoelectronic structures. It was hypothesized that the AlN(11$\bar{2}$2) layer quality improves due to a relatively slight lattice mismatch at the AlN(11$\bar{2}$2)/GaN(11$\bar{2}$2) heteroboundary.

Conflict of interest

The authors declare that they have no conflict of interest.

References

[1] A. Khan, K. Balakrishnan, T. Katona, Nat. Photon., **2**, 77 (2008). DOI: 10.1038/nphoton.2007.293
[2] R. Boichot, D. Chen, F. Mercier, F. Baillet, G. Giusti, T. Coughlan, M. Chubarov, M. Pons, Coatings, **7**, 136 (2017). DOI: 10.3390/coatings7090136
[3] Y. Iba, K. Shojiki, K. Uesugi, S. Xiao, H. Miyake, J. Cryst. Growth, **532**, 125397 (2020). DOI: 10.1016/j.jcrysgro.2019.125397
[4] Y. Yusuf, M. Samsudin, M.M. Sahar, Z. Hassan, W. Maryam, N. Zainal, Thin Solid Films, **736**, 138915 (2021). DOI: 10.1016/j.tsf.2021.138915
[5] J.-J. Wu, Y. Katagiri, K. Okuura, D.-B. Li, H. Miyake, K. Hiramatsu, Phys. Status Solidi C, **6**, S478 (2009). DOI: 10.1002/pssc.200880767
[6] M. Monavarian, A. Rashidi, D. Feezell, Phys. Status Solidi A, **216**, 1800628 (2019). DOI: 10.1002/pssa.201800628
[7] A. Mogilatenko, H. Kirmse, J. Stellmach, M. Frentrup, F. Mehnke, T. Wernicke, M. Kneissl, M. Weyers, J. Cryst. Growth, **400**, 54 (2014). DOI: 10.1016/J.JCRYSGRO.2014.04.014
[8] M. Jo, Y. Itokazu, S. Kuwaba, H. Hirayama, J. Cryst. Growth, **507**, 307 (2019). DOI: 10.1016/j.jcrysgro.2018.11.009
[9] M. Jo, Y. Itokazu, S. Kuwaba, H. Hirayama, Jpn. J. Appl. Phys., **53**, SC1031 (2019). DOI: 10.7567/1347-4065/ab0f1c
[10] L. Lahourcade, *Plasma-assisted molecular beam epitaxy of (11$\bar{2}$2)-oriented III-nitrides,* theses of PhD (Institut National Polytechnique de Grenoble, 2009).
[11] X. Luo, X. Zhang, B. Chen, Y. Shen, Y. Tian, A. Fan, Sh. Chen, Y. Qian, Zh. Zhuang, G. Hu, Mater. Sci. Semicond. Proc., **144**, 106612 (2022). DOI: 10.1016/j.mssp.2022.106612

Translated by D.Safin